Appendix A: Supplementary data

Mechanisms of heavy metal immobilization and resistance genes reduction following phosphate-modified biochar application during anaerobic digestion of swine manure

Shuo Yang[1], Qinxue Wen[2,3], Zhiqiang Chen (✉)[2,3], Ruibao Jia[1,4]

1 School of Municipal and Environmental Engineering, Shandong Jianzhu University, Jinan 250101, China

2 State Key Laboratory of Urban Water Resource and Environment, Harbin Institute of Technology (SKLUWRE, HIT), Harbin 150090, China

3 School of Environment, Harbin Institute of Technology, Harbin 150090, China

4 Jinan Municipal Water & Wastewater Monitoring Center, Jinan 250014, China

✉ Corresponding author

E-mail: czqhit@163.com

Test S1 Biochar synthesis and functional modification

For this study, wheat straw, sourced from a nearby agricultural field, served as the biochar precursor. The straw underwent pyrolysis within a controlled-temperature vacuum tube furnace. The pyrolysis process involved heating the straw to 500°C at a rate of 10°C per minute, followed by a four-hour dwell time at the target temperature. Once cooled to ambient temperature, the resulting biochar (BC) was pulverized using a mortar and then sieved to obtain particles with a diameter of less than 0.20 mm, which were reserved for subsequent experiments.

To enhance the biochar's properties, modification with phosphoric acid and potassium dihydrogen phosphate was performed. Specifically, the biochar was submerged in either a 20% H_3PO_4 solution or a 20% KH_2PO_4 solution for a 24-hour period at room temperature. The materials resulting from these treatments were labeled BP (phosphoric acid-modified) and BK (potassium dihydrogen phosphate-modified), respectively. Following the immersion, both BP and BK underwent oven-drying at 105°C overnight to yield the final biochar powders.

Test S2 The performance and changes of parameters during AD of swine manure

Table S2 details the evolution of key physical and chemical parameters during AD of swine manure, including total methane production, volatile fatty acids (VFAs), ammonium nitrogen (NH_4^+-N), total inorganic carbon (TIC), and pH. Methane yield serves as a crucial indicator of digestion efficiency. The majority of biogas production occurred within the initial 25 days of AD. The incorporation of biochar (BC, BP, and BK) enhanced the rate of methane generation during AD, resulting in significant increases in overall methane yield at the conclusion of the process. Specifically, treatments BC10, BP10, and BK10 exhibited improvements of 21.9%, 28.0%, and 35.5%, respectively, compared to the control.

Acetic, propionic, and butyric acids constitute the primary VFAs resulting from the hydrolysis and acidification of organic matter in SM. Total VFA concentrations gradually rose from 7 to 10 g/L in the early phase of digestion (approximately days 0-8), subsequently followed by the accumulation of NH_4^+-N and TIC over time (days 9-40). TIC levels fluctuated between roughly 1.2 and 5.3 g/L across all treatments. NH4 ±N and TIC acted as buffers, counteracting the buildup of VFAs and maintaining near-neutral pH levels. Throughout AD, pH values remained within an acceptable range (7.2-8.4) in all treatments, ensuring a stable environment for microbial activity.

At the end of AD, propionic acid predominated among the VFAs, while acetic and butyric acids were almost entirely depleted. The reduced total VFA content observed in biochar-amended treatments post-AD suggests efficient conversion of VFAs into methane via methanogenesis. In conclusion, all reactors functioned effectively during AD, and the inclusion of biochar (BC, BP, and BK) promoted the stability of the digestion system.

Text S3 Physicochemical analysis during AD process

The analysis of total solids (TS), volatile solids (VS), soluble chemical oxygen demand (SCOD), pH, and ammonium nitrogen (NH_4^+-N) followed established protocols (Federation and Association, 2005; Yang et al., 2021). A SHIMADZU TOC-VCPN analyzer (Japan) was employed for the quantification of total organic carbon (TOC), total nitrogen (TN), dissolved total carbon (TC), total inorganic carbon (TIC), and total alkalinity (ALK). Acetate levels were determined using a gas chromatograph (8860, Agilent, Santa Clara, USA) coupled with a flame ionization detector. Methane content was assessed via gas chromatography (7890A, Agilent, Santa Clara, USA) utilizing a thermal conductivity detector.

References

1. Federation, W. E., Association, A. P. H., 2005. Standard methods for the examination of water and wastewater. American Public Health Association (APHA), Washington, DC, USA.
2. Yang, S., Chen, Z., Wen, Q., 2021. Impacts of biochar on anaerobic digestion of swine manure: methanogenesis and antibiotic resistance genes dissemination. Bioresour. Technol. 324, 124679.

Contents

Table S1 The physicochemical characteristics of swine manure

Parameters	Swine Manure
Total solids (%)	14.17
Volatile solids (%)	7.22
pH	6.65
Soluble oxygen demand (g/L)	7.89
Ammonia nitrogen (g/L)	0.59
Total organic carbon (g/L)	14.80
Total nitrogen (g/L)	8.62
Total volatile fatty acids (g/L)	4.88

Table S2 Changes of physical and chemical parameters response to BC, BP and BK at the end of AD

Samples	Total CH_4 yield ($CH_{4(mL)}/VS_{(g)}$)	Total VFAs (g/L)	NH_4^+-N (g/L)	TIC (g/L)	pH
Control	236.49±5.19	10.06±1.71	9.89±0.37	1.24±0.22	7.4
BC10	288.33±2.44	5.95±1.03	9.01±0.46	0.91±0.05	7.8
BP10	302.78±9.72	4.60±0.26	8.49±0.71	1.42±0.04	7.8
BK10	320.35±5.67	3.24±0.51	10.40±0.74	0.97±0.12	8.1

Table S3 The primer sequences used for the identification of target genes

Genes	Target	Primer	Sequences
sul1	Sulfonamide	sul1-F	CACCGGAAACATCGCTGCA
		sul1-R	AAGTTCCGCCGCAAGGCT
sul2		sul2-F	CTCCGATGGAGGCCGGTAT
		sul2-R	GGGAATGCCATCTGCCTTGA
parC	Quinolone	parC-F	GGTGGAATATCGGTCGCCAT
		parC-R	AAACTTCGACGGCACTTTGC
aac(6')-Ib-cr		aac(6')-Ib-cr-F	GTTTGAGAGGCAAGGTACCGTAA
		aac(6')-Ib-cr-R	GAATGCCTGGCGTGTTTGA
tetG	Tetracyclines	tetG-F	GCAGAGCAGGTCGCTGG
		tetG-R	CCYGCAAGAGAAGCCAGAAG
tetW		tetW-F	GAGAGCCTGCTATATGCCAGC
		tetW-R	GGGCGTATCCACAATGTTAAC
ermB	Macrolide	ermB-F	GATACCGTTTACGAAATTGG
		ermB-R	GAATCGAGACTTGAGTGTGC
ermF		ermF-F	CGACACAGCTTTGGTTGAAC
		ermF-R	GGACCTACCTCATAGACAAG
bla$_{TEM}$	β -lactam	bla$_{TEM}$-F	ATCAGCAATAAACCAGC
		bla$_{TEM}$-R	CCCCGAAGAACGTTTTC
aadA1	Aminoglycoside	aadA1-F	CTCCGCGCTGTAGAAGTCACC
		aadA1-R	AGCGCCTCAAATAGATCCTGTTC
arsC	As	arsC -F	TCGCGTAATACGCTGGAGAT
		arsC -R	ACTTTCTCGCCGTCTTCCTT
aoxB		aoxB-F	TGCGGCTACCACGCCTACACC'
		aoxB-R	TGCCCCAGGTGTTTTCGTAAC
chrR	Cr	chrR-F	TCACGCCGGAATATAACTAC
		chrR-R	CGTACCCTGATCAATCACTT
yieF		yieF-F	CGCGGGGGCATATGTCTGAAAAATTGCAGGT

		yieF-R	TTTGGGATCCTTAGATCTTAACTCGCTGAA
pcoA		pcoA-F	CGTCTCGACGAACTTTCCTG
		pcoA-R	GGACTTCACGAAACATTCCC
copA	Cu	copA-F	TCATCGAATAGAGCCACGCC
		copA-R	CTGTGGTTGGTTATCGGCCT
cusA		cusA-F	ATGCSACVGGYGTTGGCTG
		cus-R	CCRTTCAGYTCGGCRATRCC
pbrT	Pb	pbrT -F	AGCGCGCCCAGGAGCGCAGCGTCTT
		pbrT -R	GGCTCGAAGCCGTCGAGRTA
zntA		zntA	GACTCCTGACAATCACGGCA
		zntA	GCCGGAGACGTTTTCAGAGA
czcA	Zn	czcA	CATCCCGGTGAAGGTGAACA
		czcA	TCCTGTTCCTCGGCAACATC
intI1	MGEs	intI1-F	CGAACGAGTGGCGGAGGGTG
		intI1-R	TACCCGAGAGCTTGGCACCCA
ISCR1	MGEs	ISCR-F	ATGGTTTCATGCGGGTT
		ISCR-R	CTGAGGGTGTGAGCGAG
Tn916/1545[b]	MGEs	Tn916/1545[b]-F	GACAGTATTAAGCCATCAGAC
		Tn916/1545[b]-R	TCTTCCGAACACAATCATCT
16s rRNA	Total bacteria	341F	CCTACGGGRSGCAGCAG
		806R	GGACTACVVGGGTATCTAATC

Table S4 Statistical analyses were employed to explore the interrelation between fluorescent substance intensity, HMs concentrations, and the advancement of anaerobic digestion

HMs	Component 1	Component 2	Component 3
DTPA-As	-0.289	-0.397	-0.118
As-F1	-0.37	-0.456	0.208
As-F2	0.600*	0.551	-0.051
As-F3	-0.179	-0.326	0.336
As-F4	0.159	-0.015	0.426
As-F5	-0.005	-0.373	0.537*
DTPA-Cr	-0.324	-0.366	0.143
Cr-F1	-0.532*	-0.615**	0.086
Cr-F2	0.105	0.015	0.159
Cr-F3	-0.505*	-0.522*	0.265
Cr-F4	-0.1	0.434	0.037
Cr-F5	0.434	0.147	-0.093
DTPA-Cu	0.728**	0.194	0.342
Cu-F1	-0.516*	-0.441	0.811**
Cu-F2	0.507*	0.767**	0.074
Cu-F3	-0.324	-0.532*	0.586*
Cu-F4	-0.366	-0.615**	-0.145
Cu-F5	0.143	0.086	0.132
DTPA-Pb	0.076	0.324	0.132
Pb-F1	-0.211	0.086	0.203
Pb-F2	-0.489**	-0.063	0.01
Pb-F3	0.057	0.639**	-0.044
Pb-F4	-0.226	0.394*	-0.077
Pb-F5	0.146	0.639**	0.15
DTPA-Zn	0.311	-0.25	-0.017

Zn-F1	-0.066	-0.22	-0.168
Zn-F2	0.115	0.193	0.038
Zn-F3	-0.072	0.312	-0.017
Zn-F4	0.22	-0.34	-0.168
Zn-F5	0.07	-0.33*	0.246

Table S5 2D-FTIR-COS results on the assignment and sign of each cross-peak in asynchronous maps of HCs in CK (a), BC (b), BP (c) and BK (d) treatments

(a) CK treatments						
Position (cm-1)	910	1052	1116	1256	1402	1584
910	+	+(-)	+(+)	+(-)	+(+)	+(+)
1052			+(-)	+(+)	+(-)	+(+)
1116			+	+(-)	+(-)	+(-)
1256				+	+(+)	+(+)
1402					+	+(-)
1584						+
(b) BC treatments						
Position (cm-1)	999	1115	1278	1397	1568	1700
999	+	+(+)	+(-)	+(+)	+(-)	+(-)
1115		+	+(-)	+(+)	+(-)	+(-)
1278			+	+(+)	+(+)	+(+)
1397				+	+(-)	+(-)
1586					+	+(+)
1700						+
(c) BP treatments						
Position (cm-1)	904	1082	1192	1404	1660	
904	+	+(+)	+(+)	+(+)	+(+)	
1082		+	+(+)	+(-)	+(-)	
1192			+	+(-)	+(-)	
1404				+	+(-)	
1660					+	
(d) BK treatments						
Position (cm-1)	1118	1401	1680			
1118	+	+(+)	+(+)			
1401		+	+(-)			
1680			+			

Table S6 The correlation analysis among ARGs, MRGs and MGEs during AD

Genes	aac(6')	ermF	tetG	tetW	blaTEM	aadA1	arsC	chrR	yieF	pcoA	copA	cusA	phrT	zntA	czcA	inti1	Tn916
sul1												0.495*		0.850**			
sul2	0.923*		0.862**	0.899*		0.885**		0.810**		0.902**	0.920**					0.928*	0.671*
aac(6')			0.871*	0.925*		0.86*		0.667*		0.788*	0.788**		0.563*			0.896*	0.861*
ermB		0.780**			0.528*				0.574*								
ermF					0.554*				0.533*								
tetG				0.849**		0.742**		0.721*		0.667*	0.680*		0.533*			0.831**	0.734**
tetW						0.965**	-0.501*	0.754*		0.794**	0.823*					0.970**	0.803*
blaTEM																	
aadA1								0.784**		0.864**	0.892**					0.974*	0.697**
aoxB															0.490*		
chrR										0.824*	0.861**					0.838**	
yieF												0.620**					
pcoA											0.984**					0.869**	0.505*
copA																0.898*	0.492*
phrT																	0.608**
inti1																	0.725**

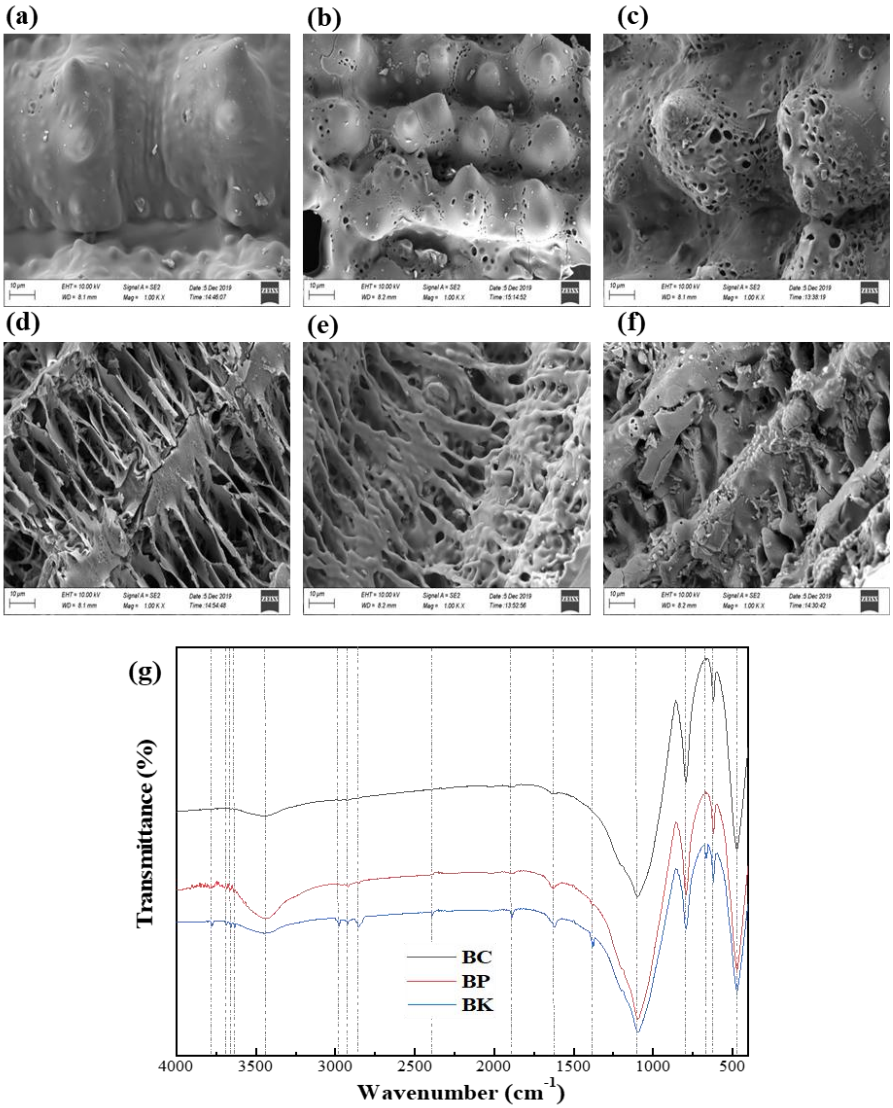

Fig. S1 SEM micrographs illustrate the morphology of BC (a, d), BP (b, e), and BK (c, f); FTIR spectroscopy was employed to characterize the pristine and modified biochar materials (g).

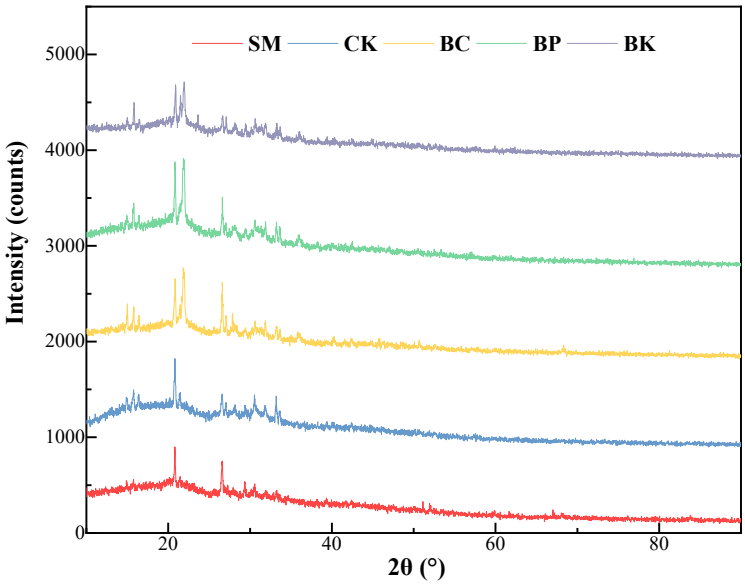

Fig. S2 XRD spectra of biochar before and after anaerobic digestion with swine manure.

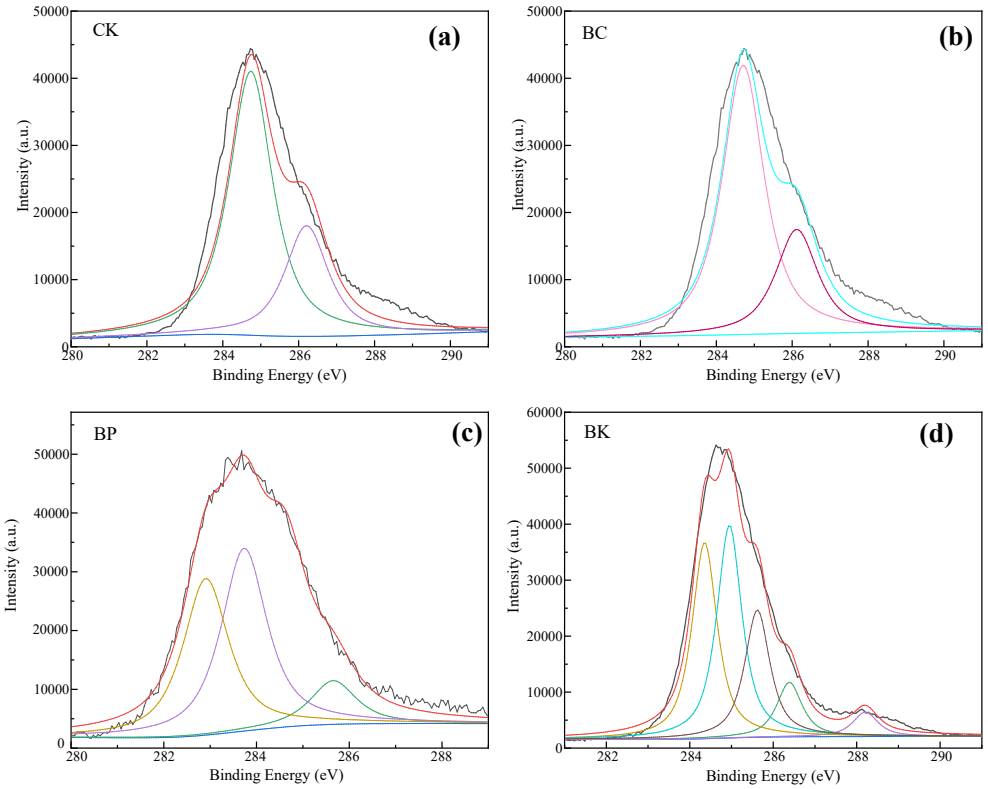

Fig. S3 High-resolution C 1s spectra reveal the carbon binding energies in the CK (a), BC (b), BP (c), and BK (d) treatment groups.

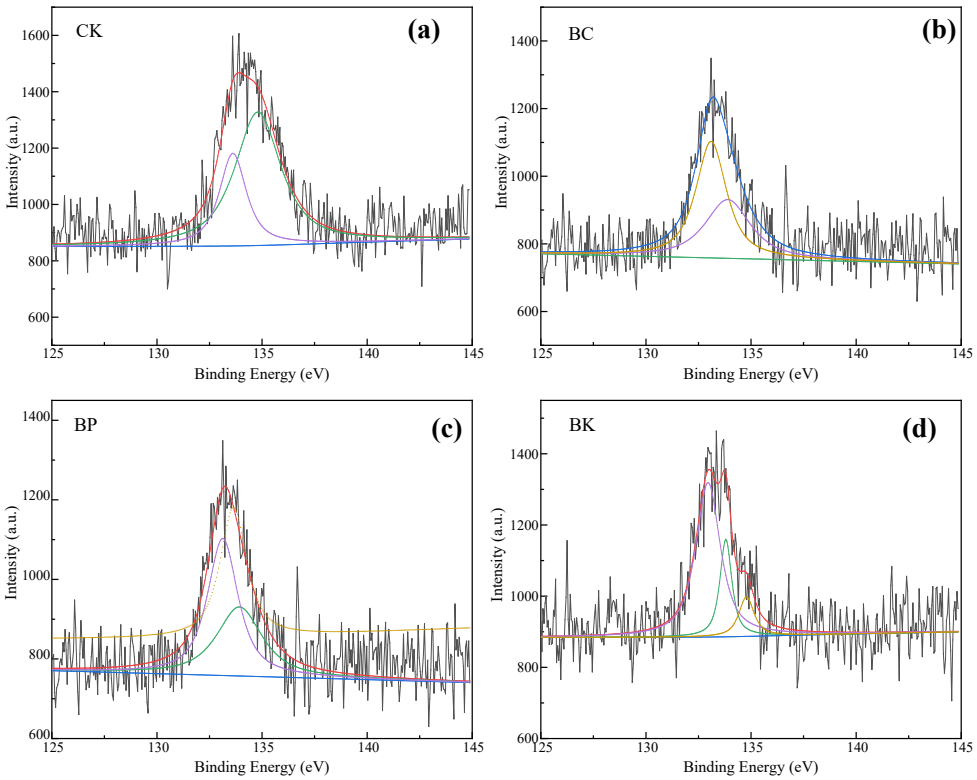

Fig. S4 The P 2p core-level spectra depict the phosphorus binding energies observed in the CK (a), BC (b), BP (c), and BK (d) treatment conditions.

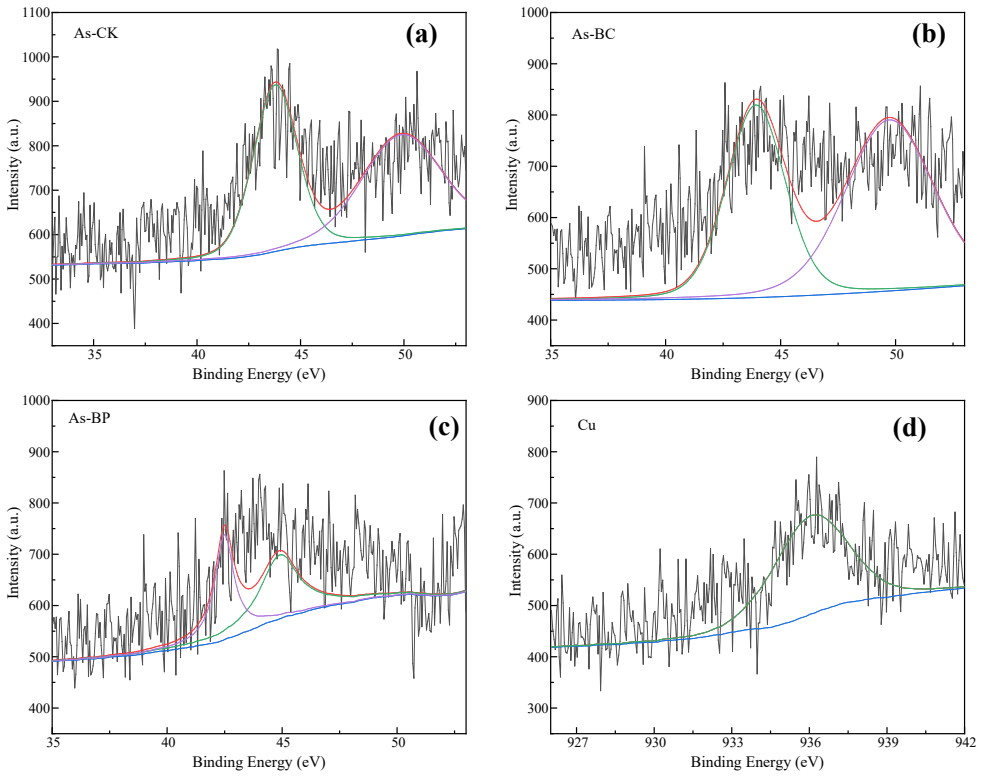

Fig. S5 The As 3d core-level spectra show the arsenic binding energies detected in the CK (a), BC (b), BP (c), and BK (d) treatment groups.

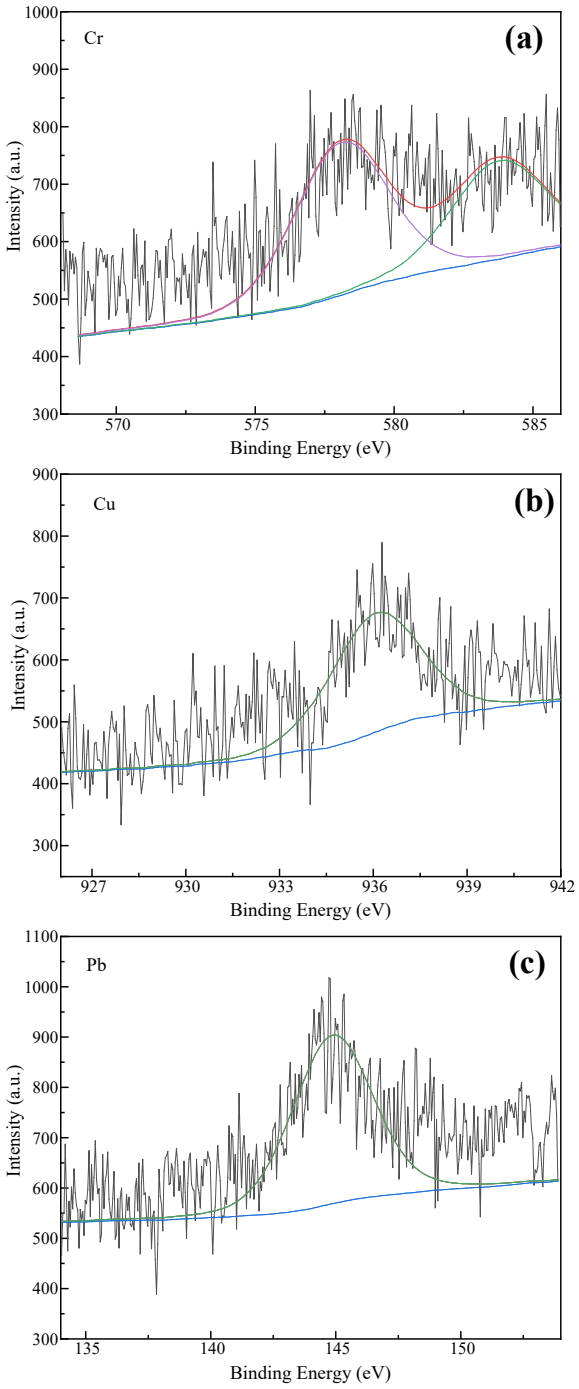

Fig. S6 Core-level spectra for Cr 2p (a), Cu 2p (b), and Pb 4f (c) were acquired to determine the binding energies of chromium, copper, and lead, respectively.